

Maria Y. Rusanova · Michail Grden
Andrzej Czerwinski · Galina A. Tsirlina
Oleg A. Petrii · Tatyana Y. Safonova

Isotope effects in α -PdH(D) as an instrument for diagnosing bulk defects

Received: 30 August 1999 / Accepted: 25 March 2000 / Published online: 16 March 2001
© Springer-Verlag 2001

Abstract Protium and deuterium sorption in the α -phase region is studied for highly defective palladium electrodeposits fabricated under controllable potentiostatic modes, particularly in the region of concentrated hydride formation. An anomalously high hydrogen content is observed for these samples in both α - and β -hydrides. On the basis of coulometry in the course of anodic hydrogen extraction, the non-linear sorption isotherms are plotted and their specific features are considered under an assumption of simultaneous equilibrium sorption of hydrogen by several types of lattice positions with a certain degree of defectiveness. Less defective palladium samples deposited in the absence of bulk hydridization are studied for comparison. The approach is proposed to estimate the fraction of defective regions. The procedure of analyzing the low-pressure limit is used for the first time for determining the specific values of the isotope effect, and also H and D Sievert's constants. The isotope effect is demonstrated to be extremely sensitive to the type of defectiveness.

Key words Palladium · Hydrides · Deuterium · Protium · Coulometry

Introduction

Among many aspects of the problem of hydrogen accumulation by solid metals at conventional pressures, an important but not always reproducible effect of

achieving anomalously high hydrogen concentrations in the β -phase of palladium should be emphasized (for example, see [1, 2, 3, 4, 5, 6]). Similar effects for the less concentrated α -phase are sufficiently well known and manifest themselves both for disordered compact [7, 8, 9, 10] and dispersed [11, 12, 13, 14] materials and, according to [7], are caused by the specific sorption properties of imperfect areas. However, in the literature, practically no data are available on comparative studies of the properties of α - and β -hydrides formed during saturation of Pd samples. This is why, to date, the questions of participation of hydrogen sorbed in defective lattice sites, during the $\alpha \leftrightarrow \beta$ transition, and the dependence of the hydrogen bulk concentration in defective areas on the H pressure (in electrochemical systems, on the potential of the palladium electrode) remain open. These questions are also important in view of fundamental science, because palladium hydrides are unique model systems for studying nonstoichiometry, one of the most important problems of the modern physical chemistry of solids. It should be noted that, along with the anomalously high hydrogen content, the lessened hydrogen content in the hydride β -phase at a high defectiveness of palladium has also been described. This result [15] concerns electrodeposits formed during simultaneous hydrogen evolution.

In this work, we consider the isotopic dependence of the bulk concentration of hydrogen during electrolytic saturation of dispersed imperfect palladium materials in solutions based on H₂O and D₂O (the question generally ignored earlier).

The studied objects are palladium deposits obtained under potentiostatic cathodic polarization. In accordance with [15, 16, 17, 18, 19], these modes ensure the formation of reproducible specific nanostructures, which demonstrate potential-dependent distributions of particles in size and texture, and also a certain bulk defectiveness. The latter property is the most pronounced when deposition proceeds in the potential region of β -phase formation under conditions when the lattice becomes deformed as a result of quick and deep

M.Y. Rusanova · G.A. Tsirlina · O.A. Petrii (✉)
T.Y. Safonova
Department of Electrochemistry, Chemical Faculty,
Moscow State University, Leninskie Gory, V-234,
Moscow, GSP-3, 119899, Russia
E-mail: petrii@elch.chem.msu.ru
Tel.: +7-095-9395501
Fax: +7-095-9390171

M. Grden · A. Czerwinski
Department of Chemistry, Warsaw University,
Zwirki i Wiguri 101, 02 089 Warsaw, Poland

hydrogenation simultaneously with its growth. For instance, some deposits formed in this case are characterized by the hydrogen concentration in the β -phase ($x_{H(\beta)}$) being higher by a factor of 1.5 compared with those known for most palladium materials [19].

Experimental

In this work, we used palladium deposits on polycrystalline gold and platinum foil electroplated from a solution of 0.06 M $\text{PdCl}_2 + 1$ M HCl under potentiostatic conditions at $E_d = -50$, 26, and 40 mV with respect to the reversible hydrogen electrode in 1 M H_2SO_4 ¹ [these types of samples are denoted below as Pd(-50), etc.; see Table 1]. In comparative experiments, we studied the deposits obtained under galvanostatic modes [denoted as Pd(gst) in Table 1] at a current density of 1 mA/cm² of the geometrical surface area. This mode corresponds to the deposition in the E_d region from 200 to 300 mV, i.e., the region of the limiting diffusion current of Pd(II) reduction at a palladium concentration of about 1 wt%, which precedes the formation of concentrated hydrides. The deposition conditions are described in more detail elsewhere [19]. The characteristic deposit thicknesses were in the submicron range.

The deposit mass m (of the order of 1 mg/cm²) was determined from the difference of the electrode masses before and after palladizing. The typical size of the electrodes was ca. 1 cm²; hence, the accuracy of the m determination could introduce a greater error in the H/Pd estimation (~10%) compared with coulometry. However, as was shown by several series of experiments with 5–7 deposits fabricated at one and the same E_d and weighed independently, the scatter in the found H/Pd data was always < 10%. Hence, the error of the m determination was systematic and at least should not affect the correctness of the comparison of the results for different deposits.

Before the experiments, the electrodes were cleaned by alternate anodic and cathodic polarization in a dilute solution of H_2SO_4 . In this case, by limiting the time of anodic polarization at $E < 1.25$ V, we could avoid dissolution of the deposit in noticeable quantities during its cleaning. The real surface areas of the electrodes, S_{Cu} and S_{O} , were determined from the adsorption of copper [20] and oxygen [21] adatoms, respectively, by measuring voltammograms in 0.5 M H_2SO_4 , including the solution with addition of CuSO_4 , from 300 mV to 1230 mV at the potential scanning rate $\nu = 1$ mV/s. For the experiments, we used fresh solutions for every electrode. In calculating S , we assumed that a charge of 420 $\mu\text{C}/\text{cm}^2$ is consumed in desorption of a monolayer of Cu adatoms and in adsorption of a monolayer of O adatoms.

It should be mentioned that the ratio of Cu desorption peaks (Fig. 1) is dependent on E_d , which can be explained by the surface texture, and the corresponding charge of the monolayer desorption should be considered as an approximate value. However, generally the uncertainty of the S_{Cu} value is in any case lower than of S_{O} , which is influenced by contributions from palladium dissolution and also from pronounced structural sensitivity of the oxygen coverage at a certain potential.

The surface images were obtained by means of a scanning tunneling microscope, whose construction and characteristics are described elsewhere [22], at a tunneling voltage of 200 mV and tunneling currents of 150–200 pA. Figure 2 shows typical images and the histograms of size distributions $j(d)$; the latter can be described under a certain approximation by the normal distribution. The position of the maximum diameter d_{max} and the distribution width depend on the deposition potential [19].

Table 1 shows the most important characteristics of the deposits studied.

Table 1 General characteristics of the Pd electrodeposits under study

Sample (E_d , mV)	$x_{H(\beta)}$ (for $E = 40$ mV)	S_{Cu} ($\text{m}^2 \text{g}^{-1}$)	S_{O} ($\text{m}^2 \text{g}^{-1}$)	d_{max} (nm)
Pd(-50)	~0.4	2.2	3.7	20
Pd(26)	~1.2	4.5	6.4	35
Pd(40)	~0.65	5.5	6.5	45
Pd(gst)	~0.65	8.0	6.2	40

The calculation of the real surface area of the deposits obtained at the potentials of hydride formation, which was carried out in accordance with the procedure of [17] with the use of STM data, provides adequate agreement with experimental S_{Cu} values [19] (however, the latter are always higher by 20–30%). At the same time, for the deposits obtained at lower overvoltages, the specific surface areas always several times exceed S_{Cu} . These deviations can stem from the fact that either the particles in the deposits merge together or the surface in narrow pores is screened. In the former case, we can refer to the formation of continuous defective areas at grain boundaries.

To determine the hydrogen content in the hydride α -phase (x_{H}), we measured the potentiodynamic curves in 0.05 M H_2SO_4 in the potential range 75–200 mV. The preliminary hydrogenation under potentiostatic conditions lasted for 20 min. The calculation of the x_{H} values was carried out by the method of Kolyadko et al. [11] by introducing a correction for the hydrogen adsorption and making an allowance for S_{Cu} . For this purpose, we used the dependence of the surface coverage by hydrogen on the potential shown in [11] for Pd black and, apparently, corresponding to somewhat overrated values. From our estimates, the corresponding error in the concentration of dissolved hydrogen can become significant (> 7–10%) only at hydrogenation potentials exceeding 200 mV.

To determine the equilibrium hydrogen content in the α - and β -phases of palladium hydrides, we measured the equilibrium charging curves [23, 24]. For this purpose, the studied palladium electrodeposit was hydrogenated under potentiostatic conditions at $E_d = 30$ mV for 6 h in a vessel bubbled with inert gas. The end of Pd bulk saturation was judged by the potential invariance after the circuit was opened. Then, after the inert gas flow was stopped, the

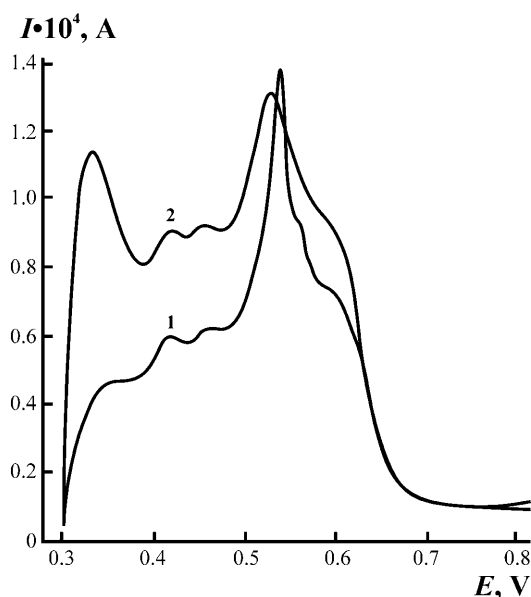


Fig. 1 Cyclic voltammograms of Cu desorption obtained in 0.5 M $\text{H}_2\text{SO}_4 + 0.1$ M CuSO_4 solution after formation of a monolayer at $E = 300$ mV for Pd deposited on Au at $E_d = -50$ (1) and 40 (2) mV

¹ In the experiments, we also used a silver-silver chloride electrode. All the E values are given on the reversible hydrogen electrode (RHE) scale

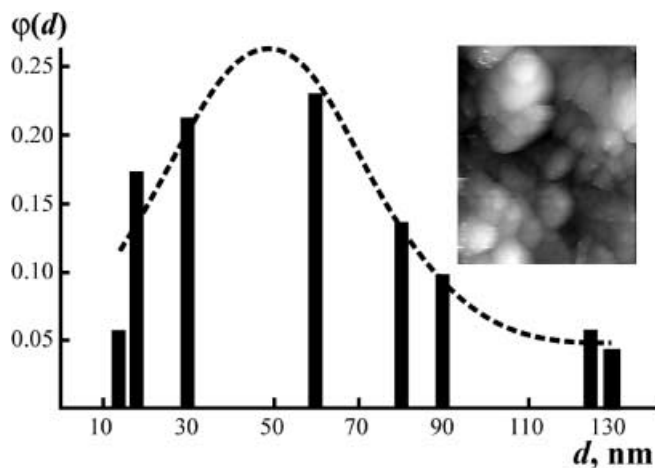


Fig. 2 Typical STM image of electrodeposited Pd ($180 \times 214 \text{ nm}^2$) and size distribution constructed from statistical treatment of a set of images for Pd(40)

electrode was polarized anodically under galvanostatic mode at current densities of $0.1\text{--}1 \text{ mA/cm}^2$ of the geometrical surface area (high current values were used only in the region of the $\alpha \leftrightarrow \beta$ transition) and the time dependences of the potential were recorded. The circuit was periodically opened and the potential was left to shift to the constant value. Thus, we obtained the dependence of the equilibrium potential values on the charge passed.

In this work, we used the solutions prepared from twice distilled H_2SO_4 (18 M), HCl (6 M), and water. The deuterated reagents were purified in the same fashion (for details, see [23, 24]). The solutions were deaerated by argon purified from oxygen traces. The electrochemical measurements were carried out in an automatic mode by means of potentiostat-galvanostat CHI 604 (Cordoba, USA) controlled by an IBM compatible Pentium computer. The potential E of the working electrode was measured with respect to the RHE in aqueous $0.5 \text{ M H}_2\text{SO}_4$. The pH of this solution (0.5) differed from that of deposition solutions (0.4). The corresponding correction for the potential value with respect to the RHE (the scale used in [18]) in the deposition solution was about 6 mV. The correction for the difference of equilibrium hydrogen potentials in protium and deuterium media (4 mV) was introduced when the pressure dependences were calculated and has been discussed in detail previously [23, 24].

Results

Experimental studies of the protium-deuterium isotopic effect at the formation of equilibrium $\alpha\text{-PdH}_x$

The effective diffusion coefficients of protium and deuterium atoms are influenced by a large number of structural properties of polycrystalline materials, and, to obtain reliable sorption data, the technique of equilibrium charging curves [25] is most suitable. As an example, Fig. 3 compares the coulometric data obtained on a Pd(26) sample under equilibrium conditions with voltammetric results at $v = 1\text{--}5 \text{ mV/s}$.

² Actually, from here on, we consider the defective materials as the equilibrium phases of a special structure, because the lifetime of long-lived metastable defects in the considered electrodeposits far exceeds the time necessary for equilibrium to be reached for the processes with participation of hydrogen. It is in this sense that the term "sorption isotherm" is applied to such quasi-equilibrium materials

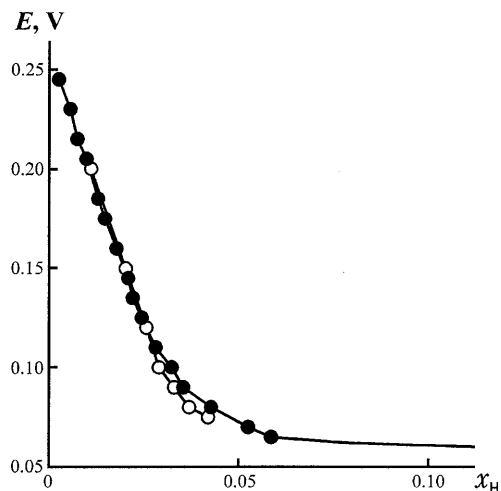


Fig. 3 Equilibrium charging curve for Pd(26) (solid symbols) and the values of α -phase hydride concentration obtained by potentiodynamic extraction (open symbols)

Below, when analyzing the segment of the sorption isotherm² for $\alpha\text{-PdH(D)}_x$, we mainly use the results obtained during potentiodynamic extraction, which, as follows from Fig. 3, correspond to equilibrium extraction of hydrogen at $E < 0.085\text{--}0.090 \text{ V}$. Figure 4 shows the dependences of the hydride concentration $x_{\text{H(D)}}$ on the potential on the traditional coordinates x vs. $p^{1/2}$ [26] (effective hydrogen pressure p is calculated from the saturation potential via the Nernst equation). For all the samples studied, in contrast to bulk polycrystalline palladium with a micron grain size (curves 1, 1', Fig. 4), the isotherms are characterized by a pronounced non-linearity and substantially above (in a number of cases, by an order of magnitude and higher) concentrations of

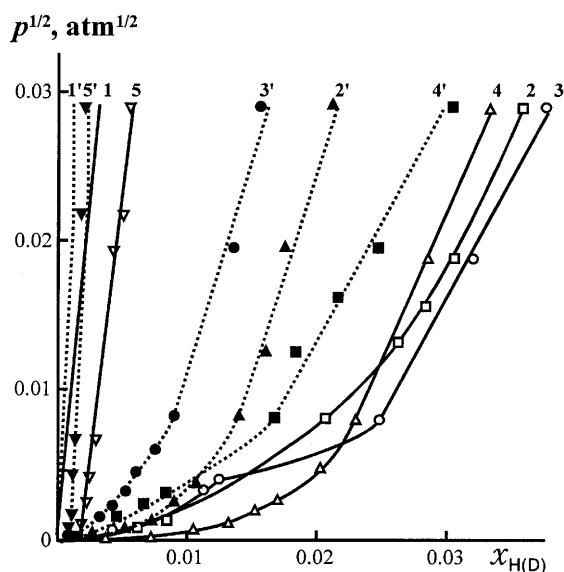


Fig. 4 Hydrogen sorption isotherms in the α -phase region. Curves 1–5 correspond to x_{H} , curves 1'–5' to x_{D} . 1, 1': smooth polycrystalline Pd [26]; 2, 2': Pd(–50); 3, 3': Pd(26); 4, 4': Pd(40); 5, 5': Pd(gst)

hydride, especially at low p . This behavior is typical for disordered materials, in whose lattice the defects work as hydrogen traps [7, 8, 26, 27].

Owing to significant differences in the isotherm slopes, the ratio of the hydride concentration for different deposits is pressure dependent. Moreover, the reproducibility of concentrations of dissolved hydrogen for the same E_d is substantially lower compared with structural and adsorption characteristics, which is quite understandable because the formation of nonequilibrium defects in the material bulk depends on quite a number of factors which are difficult to control. We can outline only certain tendencies of the E_d effect on the sorption behavior, which are discussed in detail in Rusanova et al. [19].

Palladium electrodeposits obtained at “medium” deposition potentials (250–400 mV) are represented in this study by Pd(gst). The similarity of their structure and sorption properties was discussed in detail in Rusanova et al. [19]. For these types of deposits, the excess low-pressure concentrations are always lower and the isotherm slopes ($dp^{1/2}/dx$) at the region of quasi-linear behavior are always higher compared with deposits obtained at the potentials of concentrated hydride formation. For the latter, the equilibrium potential of the $\alpha \leftrightarrow \beta$ transition proves to be somewhat lower. Anomalous high hydrogen concentrations in the β -phase are observed only for a narrow E_d interval close to 20 mV.

At a constant pressure (constant potential), on all the deposits, the values of x_D obtained in deuterium media appear to be lower than the corresponding concentrations of protium x_H . The dependences of the ratio x_D/x_H on the pressure for the samples studied in this work differ significantly from one another and also differ from the literature data for compact palladium materials [26, 28] (see below).

In certain isotherms of Fig. 4, at a $p^{1/2}$ of about $0.005 \text{ atm}^{1/2}$ ($E = 130\text{--}140 \text{ mV}$), a bending appears; however, the analysis of its nature is beyond the scope of this work. It cannot be ruled out that it arises as a result of insufficiently accurate corrections for the hydrogen adsorption, for example, owing to the presence of hydrogen adatoms in a certain characteristic state, which desorb in a narrow potential region (the charge for hydrogen adatom desorption is comparable with the charge of α -hydrogen desorption at $p^{1/2} < 0.005 \text{ atm}^{1/2}$). One cannot also exclude the realization of a phase transition similar to the $\alpha \leftrightarrow \beta$ transition in the regular lattice when the high degree of occupation of defective positions arranged in large compact groups is reached.

Coulometric analysis of potentiodynamic curves of protium and deuterium desorption (Fig. 5) served as the basis for plotting the isotherms under discussion. As was discussed in detail in Rusanova et al. [19], these curves

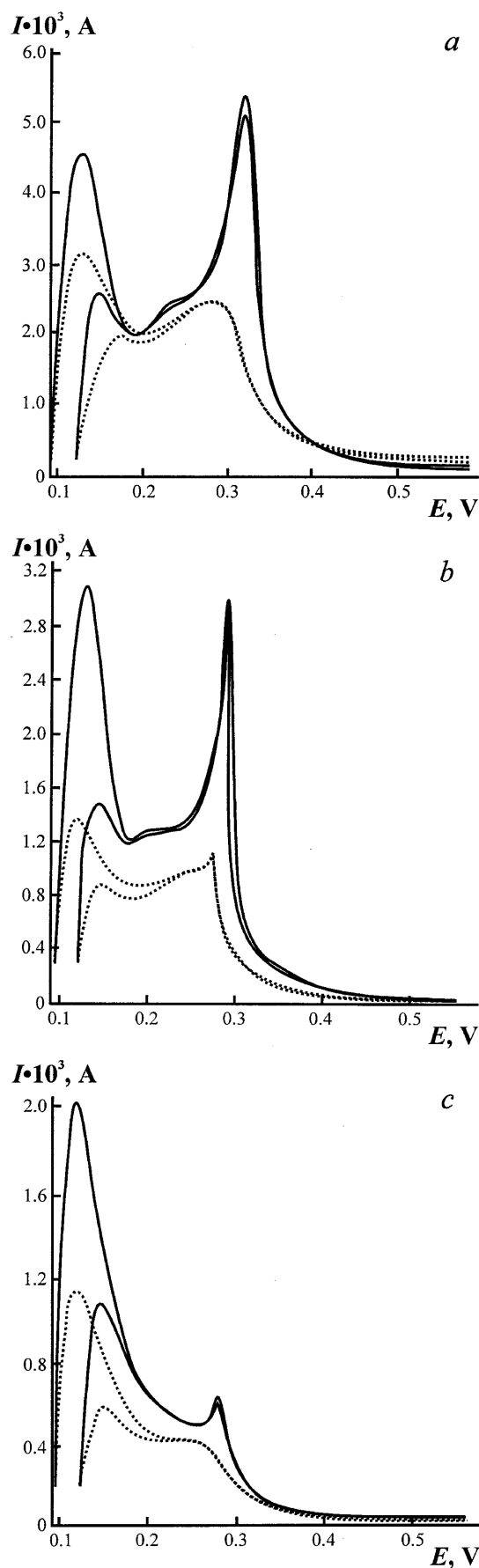


Fig. 5 Typical potentiodynamic curves obtained in the course of extraction after hydride (deuteride) saturation at $E = 90$ and 120 mV : **a** Pd(-50), **b** Pd(26), **c** Pd(40); *solid lines* correspond to protium and *dashed lines* to deuterium extraction

Table 2 Potentials and relative heights of peaks in voltammograms measured during hydrogen extraction after hydrogenation at $E=0.09$ V (the values of currents I are normalized to the height of the highest current peak)

Sample	E (mV)/ I	E (mV)/ I	E (mV)/ I	E (mV)/ I	E (mV)/ I
Pd(-50)					
Protium	120/0.85	–	220/0.46	270/0.65	290/1.00
Deuterium	125/1.00	–	215/0.70	255/0.79	–
Pd(26)					
Protium	115/1.00	190/0.38	217/0.42	260/0.53	280/0.97
Deuterium	100/1.00	–	240/0.74	260/0.83	–
Pd(40)					
Protium	115/1.00	–	–	–	275/0.30
Deuterium	115/1.00	200/0.38	220/0.36	–	–
Pd(gst)					
Protium	105/1.00	–	–	260/0.10	–
Deuterium	110/1.00	–	240/0.12	270/0.10	–

correspond to equilibrium desorption, if the saturation potential is above 0.09 V. The equilibrium was confirmed by the coincidence of the charge on anodic and cathodic curves at a given sweep rate, and also by the coincidence with the data of equilibrium charging curves.

The complicated shape of the current peaks in Fig. 5 can point probably to the existence of different forms of extracted hydrogen. The comparison of the data for the same samples in solutions of different isotope composition shows that, at a constant saturation potential, the regions of protium desorption are wider compared with deuterium. In a number of cases the desorption peak corresponding to the most strongly bound state is observed only for the lighter isotope. Table 2 shows the relative heights and potentials of the peaks.

It is probable that relatively weakly pronounced features correspond (at least partly) to desorption of hydrogen adatoms. At the same time, at least two (and in certain cases even three) characteristic peaks correspond to the charges that are known to be higher than the charge of desorption of a hydrogen monolayer [12, 29], and can be assigned only to certain hydrogen states in the hydride bulk, for example in the most defective and most regular lattice fragments.

We do not consider in this paper the other possible reason for the appearance of the specific anodic feature at ca. 0.28 V [30]. Generally, this probability cannot be ignored; however, the modes of pretreatment that induced this interesting effect [30] are highly specific and differ strongly from the modes used in our study. For exact clarification of this problem, direct chemical analysis of both hydrogen in bulk Pd and oxygen on the surface is necessary.

In the next section, we make an attempt to consider the hydrogen sorption as an additive process of parallel saturation of defective and defectless areas.

Model analysis of sorption isotherms

In earlier literature, when analyzing the processes of hydrogen sorption with participation of defective metals

and alloys, authors mainly used the Oriani approach [31], which generalized earlier attempts to consider the equilibrium between the sorbed atoms with different binding energies. In Bucur [7], to describe the equilibrium hydrogen concentrations in palladium materials, the model of Oriani [31] was used, which allows one to reduce the treatment of experimental data to a graphical determination of the Sievert's constant K_s (from the slope of the isotherm segment in the higher pressure region) and the share of lattice defects r_t^0 (by extrapolating the aforementioned region to $p=0$):

$$x_H = r_t^0 \frac{\sqrt{p_{H_2}}}{K + \sqrt{p_{H_2}}} + \frac{\sqrt{p_{H_2}}}{K_s} \quad (1)$$

Further analysis with the use of these parameters allows one, in accordance with [7], to obtain also the values K , which can be considered as the effective Sievert's constants for defective areas (in accordance with [7], these are the constants of the equilibrium between hydrogen in defective and defectless positions normalized to K_s). Table 3 shows the results of formal treatment of the data of Fig. 4 in accordance with Eq. 1. The accuracy of K_s determination differs for different samples and, as a rule, is low owing to the narrowness of the linear segment.

An adequate description of the region of medium compositions by Eq. 1 for most electrodeposits discussed could not be achieved at any K values. At the same time, typical values of r_t^0 for all deposits lie in the same interval as those of the samples studied in [7], and also for those electrodeposited and obtained by chemical reduction of palladium from its solutions [11, 12, 13, 14]³. We made an attempt to compare the values found by us and also by others [11, 12, 13, 14, 15, 16, 17] with K_s vs. r_t^0 dependence plotted in [7] (Fig. 6). The solid curve in Fig. 6 taken from [7] practically flattens out in the interval of relatively high r_t^0 typical of electrodeposits. In this case, the scatter in the values

³ In the last case, the applicability of Eq. 1 was checked only in a narrow region of pressures [12], and the corresponding K values were not presented

Table 3 Parameters of Eq. 1 for the palladium samples studied

Sample	K_s (atm ^{1/2}) (H/D)	K (atm ^{1/2}) (H/D)	r_t^0 (H/D)	$(x_H/p^{1/2})_{p \rightarrow 0}$	$(x_H/x_D)_{p \rightarrow 0}$
Pd(-50)	3.1/3.9	—	0.019/0.015	~20	2.4
Pd(26)	~2/~3	—	0.018/0.008	~10	2.4
Pd(40)	2.2/1.7	—	0.015/0.008	~10	~2
Pd(gst)	5.6/18	—	0.001/0.001	~2	1.3
Smooth [25]	12/24	—	< 10 ⁻⁴	0.08	2.05
Typical values [6]	2–20	~1	10 ⁻⁴ –10 ⁻²	—	—

corresponding to dispersed Pd is sufficiently wide. Undeniably, in this case, we can speak only of a certain correlation, because, at least at low bulk concentration of hydrides, the individual properties of defective areas and those with a lesser number of defects (which is described by the value K_s) cannot depend on the presence of positions of different types in the imperfect samples. Indeed, Sievert's law in its simplified form ($x_{H(D)} \approx p^{1/2}$), which can be applied only to very diluted hydride phases [26], assumes the absence of long-range effects (particularly, hydrogen-hydrogen interactions). If we build the K_s vs. r_t^0 dependence for electrodeposited Pd only, it is difficult to find any systematic correlation.

For the same reason, the presence in these materials of continuous truly perfect areas should be called into question. Were the fraction of regular structural fragments really substantial, then, after occupation of all the defective vacancies in a certain pressure interval, the dependence of the composition on $p^{1/2}$ should be expected to be linear with a slope K_s equal to the value known for virtually defectless (coarsely crystalline, annealed) palladium (at room temperature, about

12 atm^{1/2} [26, 32]). As follows from our data [19], the significantly lower values of K_s determined by the usual linear approximation of isotherm segments at $p^{1/2} < 0.03$ – 0.04 atm^{1/2} are not the result of the error associated with the narrowness of the interval considered. On the contrary, when the interval is widened to 0.08 atm^{1/2} [19], the values of K_s appear to be still lower (< 1 atm^{1/2}). Thus, in the imperfect materials studied in [7] and in this work, either the defectless areas are altogether absent, or several types of defects are present with the overall concentration substantially higher than r_t^0 so that the contributions of perfect areas do not prevail up to the region of the $\alpha \leftrightarrow \beta$ transition.

Indeed, this question cannot be solved without studying independently and in detail the nature of defects (in [7, 8], they were characterized as dislocations, and in [12] the role of lattice vacancies was emphasized). Along with these suppositions, the possible contributions of defective areas of more complicated structure [9] also need to be thoroughly checked; first of all, anomalous areas of intergranular boundaries. The latter are considered responsible, for example, for the sorption of excessive hydrogen by palladium compacts (the materials obtained under pressure from powders [10]).

The conditional way of characterizing the fracture of defective positions by the parameter r_t^0 in Eq. 1 should be called into question, bearing in mind the isotopic dependence found for this parameter (Table 3). The r_t^0 values obtained from the isotherms of Fig. 4 on the basis of Eq. 1 formally suggest that the number of defects that can be occupied by protium far exceeds the number of potential positions for the strongly bound deuterium. However, the sizes of protium and deuterium atoms differ insignificantly, and the sorption of the latter should not cause any steric hindrance. It is more probable that the precision of determination of the number of "special" sites by using linear extrapolation in a narrow pressure interval is unsatisfactory.

In the context of estimating the possible proportions of defect concentrations, it should be noted that, for quite a number of different palladium materials, the sorption isotherms in the β -phase are described by the same logarithmic x_H vs. $\ln p$ relationships [25, 26, 33], which allows one to assign the corresponding parameters of isotherms to a defectless lattice. It is obvious that, at a low bulk content of defective positions, it is difficult

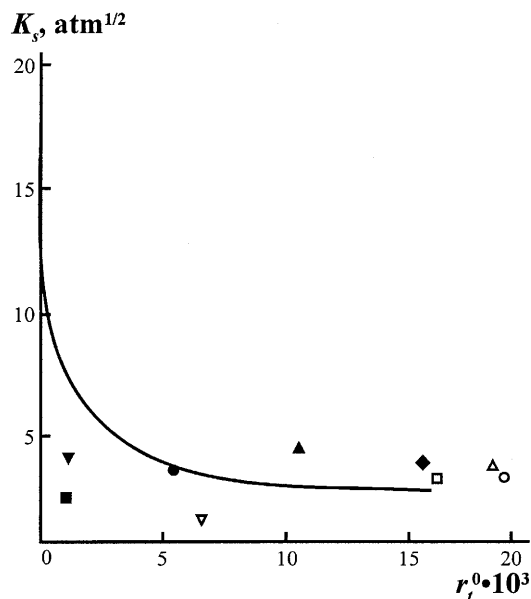


Fig. 6 K_s vs. r_t^0 dependence reported in [7] for disordered Pd foils (solid curve) and corresponding points for electrodeposited Pd (protium, open symbols; deuterium, solid symbols)

to experimentally detect their contribution to the value of x_H for concentrated hydrides which is comparable with unity. This is why the aforementioned deviations of concentrations in the β -phase both to higher and lower values [19] (Table 1) can be considered as an indication of a low bulk content of precisely defectless lattice fragments in the corresponding materials. In the sample Pd(-50) the numerous defective positions probably tend to form concentrated hydrides at high pressures, compared with equilibrium palladium lattice, whereas in the sample Pd(26) this proceeds at low pressures. The decrease in the β -phase concentration, compared with that formed by "usual" Pd, was also found in [34] for bright Pd deposited from H_3PO_4 -containing solutions at high current densities.

When analyzing defective materials within the framework of Eq. 1, it is necessary to bear in mind that the constant K can depend on the hydrogen concentration. According to [7], the fact that the dependence x_H vs. p approaches a straight line points to the limiting occupation of defective positions. If such an assumption is made for the defective positions arranged in compact groups (for example, in the region of intergrain boundaries), then interactions of hydrogen atoms in closely localized positions inevitably change the effective value of K . The variation of K with x_H is usually taken into account in Sievert's law by introducing the factor that depends on x_H [26]. The dependence of K on the concentration of defects was also mentioned in [30]; moreover, it was detected experimentally for dislocation traps (catchers) arranged at sufficiently far distances from one another.

Considering the dependence of K on the composition is, in principle, similar to considering the set of n types of the i th defect areas in the material bulk with the partial volume content N_i , while the individual desorption peaks can result from the changes in the hydrogen state in the positions of the same type induced by the changes in concentration.

In future studies, it seems challenging to carry out a special analysis of complicated sorption isotherms by assuming that the areas of different types are additive and on the basis of classical relationships [26] with partial Sievert's constants K_i and K_i^* for H and D, respectively, i.e.:

$$x_H = \sqrt{P_{H_2}} \sum_{i=1}^n \frac{N_i}{K_i + \sqrt{P_{H_2}}}, \quad x_D = \sqrt{P_{D_2}} \sum_{i=1}^n \frac{N_i}{K_i^* + \sqrt{P_{D_2}}}, \quad \sum_{i=1}^n N_i = 1 \quad (2)$$

In contrast to Eq. 1, Eq. 2 is suitable also for the cases where the concentration of defective positions is comparable with 1, and also for an arbitrary region of pressures and any type of defect space distribution. They correspond to the condition that an equilibrium exists between hydrogen in the gas phase and in every type of defect position, which is equal to the equilibrium condition considered by Bucur [7] and Oriani [31].

At $p \rightarrow 0$, Eqs. 2 are transformed into the following form:

$$\frac{x_H}{\sqrt{P_{H_2}}} = \sum_{i=1}^n \frac{N_i}{K_i}, \quad \frac{x_D}{\sqrt{P_{D_2}}} = \sum_{i=1}^n \frac{N_i}{K_i^*}, \quad \sum_{i=1}^n N_i = 1 \quad (3)$$

If one of the terms in Eq. 3, N_i/K_i , is substantially higher than the other terms, then the limiting value $x/p^{1/2}$ in fact characterizes the only type of position: defective areas most abundant and/or characterized by the strongest bonds. Such a value can be found by extrapolation of the coordinates $x/p^{1/2}$ vs. $p^{1/2}$. Such a procedure for analyzing the experimental data is shown in Fig. 7, and the values found by extrapolation are given in Table 3.

On the simplest assumption that only two types of lattice position are present ($n=2$, $N_1=N$, $N_2=1-N$), then Eqs. 3 take the following form:

$$\left(\frac{x_H}{\sqrt{P_{H_2}}}\right)_{p \rightarrow 0} = \frac{1-N}{K_2} + \frac{N}{K_1}, \quad \left(\frac{x_D}{\sqrt{P_{D_2}}}\right)_{p \rightarrow 0} = \frac{1-N}{K_2^*} + \frac{N}{K_1^*} \quad (4)$$

and if $N \ll 1$, one can simply put 1 in the numerators of the first term on the right-hand side and obtain the low-pressure limit of Eq. 1, K_2 and K_2^* having a meaning of K_s for H and D. Considering the first type (K_1 , K_1^*) as the more defective trapping positions, and the second one (K_2) as the less defective, we can assume on a good approximation that K_1 is small compared with K_2 . At the same time, in accordance with the data of Fig. 6 for K_s (which may be underrated), $(1-N)/K_2$ is close to $1/K_2$ and smaller than 1 (in the limiting case, 0.05), i.e., the main contribution to the high limiting values of $(x/p^{1/2})$ (Table 3) is made by the term N/K_1 . In as much as $N < 1$, the maximum possible K_1 are 0.02–0.05 for small N , and are by several orders of magnitude smaller for N really

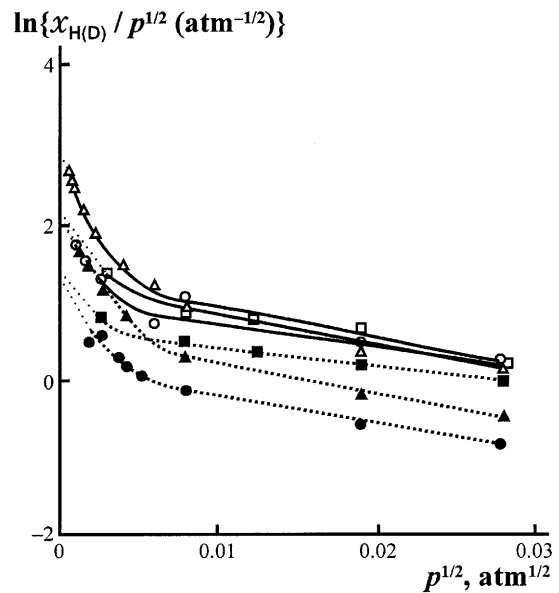


Fig. 7 The analysis of the low-pressure limit in accordance with Eq. 4 for Pd(-50) (triangles), Pd(26) (circles), and Pd(40) (squares). Open symbols correspond to x_H , solid symbols to x_D

close to the formal values of r_1^0 . In any case, the effective Sievert's constants for imperfect areas at a zero pressure are by several orders of magnitude higher than the characteristic values shown in [7].

The impossibility to approximate the experimental data of Fig. 4 in the overall p interval by Eq. 1 results precisely from the existence of a pronounced dependence of K on x . In the samples discussed in [7], a substantial delocalization of defects probably took place, which weakened the interaction of strongly bound hydrogen atoms and provided a weak dependence of K on the concentration.

To find the dependence of K on x on the basis of data for two hydrogen isotopes is a challenge. This would have been possible in principle within the framework of the model of two types of sorption positions for the separation coefficients H/D (a) independent of the defect nature. Then, the known relationship $K_i^* = a^* K_i$ would have ensured the independent calculation of both N and K_1 by using Eqs. 4. However, realization of this calculation procedure requires precise data on the equilibrium compositions in an interval as wide as possible for both low and high p , while the fulfillment of the required conditions is, apparently, possible only for certain types of palladium materials. Particularly, on the basis of the data of this work, we can assume that a depends on the position type.

Indeed, in accordance with Eqs. 3, at $p \rightarrow 0$ the ratio x_H/x_D characterizes the specific isotopic effect $a = K_i/K_i^*$ only for one of n position types (the type for which the ratio N_i/K_i is maximum).

At low p (Fig. 8), at least for Pd(26) and Pd(-50) samples, the x_H/x_D values tend to the same value of 2.4–2.5, i.e., far exceed x_H/x_D for all compact palladium materials measured in the region of the α -phase at room temperature (1.95–2.17 [26], horizontals on Fig. 8 mark the boundaries of this region). For a deposit obtained beyond the hydrogenation region, x_H/x_D decrease with decreasing p and tend to 1.2–1.3. The detection of the specific isotope effects requires additional measurements in the region of low pressures.

Conclusions

Highly defective samples of electrodeposited Pd studied in this work are characterized by equal concentrations of protium in the hydride α -phase (curves 2–4 in Fig. 4). At the same time, isotopic H/D effects for the corresponding hydrides (Fig. 8), both limiting ones (at low pressure) and (first of all) in the whole studied region of pressures, display substantial differences in the sorption behavior of different materials, which is also indicated by the β -hydride concentrations determined in [19].

The prospects of using the properties of concentrated hydrides for indirect structural diagnostics are hardly high today owing to complications and the approximate

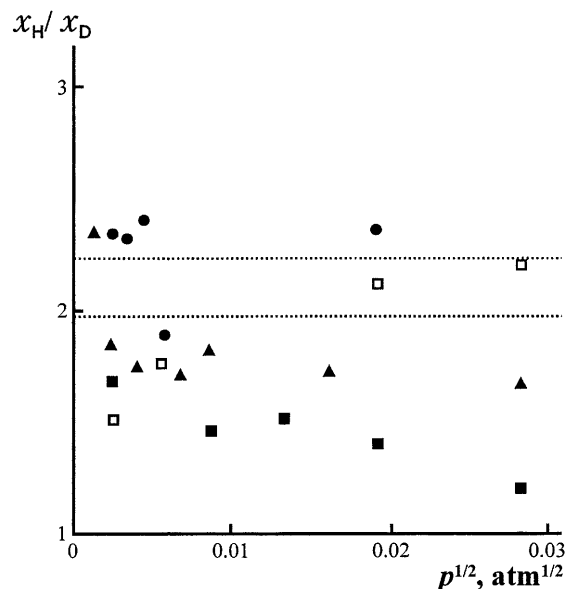


Fig. 8 Pressure dependence of the sorption isotope effect for the α -phase (x_H/x_D). The area marked by horizontal lines corresponds to the pressure-independent values for perfect Pd [26]. Solid symbols: Pd(-50) (triangles), Pd(26) (circles), and Pd(40) (squares). Open squares: Pd(gst)

nature of the corresponding theoretical descriptions. At the same time, for a hydride phase, an unambiguous relationship exists between the isotope effect and the oscillatory modes of hydrogen and deuterium in the lattice, which gives grounds to expect that in future the definite quantitative characteristics will be found for different types of defective regions.

Whereas the studies of the adsorption of metal atoms on Pd can serve as a simple tool for finding the dependence of the surface structure on the conditions of deposit fabrication, the comparison of the sorption of protium and deuterium, as was shown above, characterizes, first of all, the analogous specific features of solid state properties. It is interesting that a certain parallelism is observed between the changes of surface and bulk properties. This allows us to hope that the approaches to solving one of the most important problems of solid state electrochemistry – the relationship between bulk and surface characteristics of electrode materials – will be developed.

One should also take into account the anomalous pressure dependences of the isotope effect for imperfect palladium when constructing membrane reactors and separators. Membrane devices exploit palladium foil modified by dispersed (particularly electrodeposited) palladium, which can result in a pronounced decrease of the separation factor in a certain pressure range.

Acknowledgements The study was partly supported by the Russian Foundation of Basic Researches, project no. 99-03-32341a. A contribution from the University of Warsaw for M.R. is also acknowledged. The authors are grateful to Dr. Sergey Vassiliev for his kind help with the STM imaging of samples.

References

1. Riley AM, Seader JD, Pershing DW (1992) *J Electrochem Soc* 139:1342
2. Green TA, Quickenden TI (1994) *J Electroanal Chem* 368:121
3. McKubre MCH, Crouch-Baker S, Rocha-Filho RC, Smedley SI, Tanzella FL, Passell TO, Santucci J (1994) *J Electroanal Chem* 368:55
4. Mengoli G, Bernardini M, Fabrizio M, Manduchi C, Zannoni G (1996) *J Electroanal Chem* 403:143
5. Wark A, Crouch-Backer S, McKubre MCH, Tanzella FZ (1996) *J Electroanal Chem* 418:1999
6. Bernardini M, Comisso N, Tabrizo M, Mengoli G, Randi A (1998) *J Electroanal Chem* 453:221
7. Bucur RV (1987) *J Mater Sci* 22:1402
8. Bucur RV (1987) *Acta Metall* 35:1325
9. Wert CA (1978) In: Alefeld G, Volkl J (eds) *Hydrogen in metals, part II*. Springer, Berlin Heidelberg New York, chap 8
10. Eastman JA, Fitzsimmons MR, Muller-Stach M, Wallner G, Elam WT (1992) *Nanostruct Mater* 1:47
11. Kolyadko EA, Shigan Lu, Podlovchenko BI (1992) *Elektrokhimiya* 28:385 [in Russian]
12. Podlovchenko BI, Kolyadko EA, Shigan Lu (1995) *J Electroanal Chem* 399:21
13. Shigan Lu, Kolyadko EA, Podlovchenko BI (1993) *Russ J Electrochem* 29:403
14. Shigan Lu, Kolyadko EA, Podlovchenko BI (1993) *Russ J Electrochem* 29:408
15. Podlovchenko BI, Petukhova RP, Kolyadko EA, Lifshits AD (1976) *Elektrokhimiya* 12:813 [in Russian]
16. Podlovchenko BI, Petukhova RP (1970) *Elektrokhimiya* 6:198 [in Russian]
17. Petrii OA, Tsirlina GA, Pron'kin SN, Spiridonov FM, Khrushcheva ML (1999) *Russ J Electrochem* 35:8
18. Gamburg YuD, Petukhova RP, Lifshits AD, Podlovchenko BI, Polukarov YuM (1979) *Elektrokhimiya* 15:1875 [in Russian]
19. Rusanova MYu, Tsirlina GA, Petrii OA, Safonova TYa, Vassiliev SYu (2000) *Russ J Electrochem* 36 (in press)
20. Maksimov YuM, Lapa AS, Podlovchenko BI (1989) *Elektrokhimiya* 25:712 [in Russian]
21. Breiter MW (1977) *J Electroanal Chem* 81:275
22. Vassiliev SYu, Denisov AV (2000) *Zh Tekhnicheskoi Fiz* (in press) [in Russian]
23. Tsirlina GA, Rusanova MYu, Petrii OA (1993) *Russ J Electrochem* 29:412
24. Tsirlina GA, Rusanova MYu, Roznyatovskii VA, Petrii OA (1995) *Russ J Electrochem* 31:20
25. Fedorova AI, Frumkin AN (1953) *Zh Fiz Khim* 27:247 [in Russian]
26. Wicke E, Brodowski H (1978) In: Alefeld G, Volkl J (eds) *Hydrogen in metals, part II*. Springer, Berlin Heidelberg New York, chap 2
27. Kirchheim R (1980) *Scr Metall* 14:905
28. Oates WA, Lasser R, Kuji T, Flanagan TB (1986) *J Phys Chem Solids* 47:429
29. Szpak S, Mosier-Boss PA, Scharbor SR (1992) *J Electroanal Chem* 337:147
30. Burke LD, Nagle LC (1999) *J Electroanal Chem* 461:52
31. Oriani RA (1970) *Acta Metall* 18:147
32. Bruners RU, Maksimov YuM, Podlovchenko BI (1986) *Elektrokhimiya* 22:264 [in Russian]
33. Perminov PS, Orlov AA, Frumkin AN (1952) *Dokl Akad Nauk SSSR* 84:749 [in Russian]
34. Bucur RV (1970) *J Electroanal Chem* 25:342